Adsorption and Decomposition of 1-Alkanethiols on the Fe(100) Surface

Longchun Cheng, Steven L. Bernasek,* and Andrew B. Bocarsly*

Department of Chemistry, Princeton University, Princeton, New Jersey 08544

T. A. Ramanarayanan*

Corporate Research Laboratories, Exxon Research and Engineering Company, Annandale, New Jersey 08801

Received December 16, 1994. Revised Manuscript Received July 5, 1995[⊗]

The adsorption and decomposition of 1-alkanethiol molecules ($C_nH_{2n+1}SH$, $n = 4, 6, 10$) on the Fe(100) surface under ultrahigh vacuum have been investigated using temperature-programmed reaction spectroscopy (TPRS), Auger electron spectroscopy (AES), low-energy electron diffraction (LEED), and high-resolution electron energy loss spectroscopy (HREELS). Upon adsorption at 100 K, 1-alkanethiol molecules undergo S–H bond scission to form a surface alkanethiolate ($-SC_nH_{2n+1}$). The alkanethiolate starts to decompose below 255 K via C–S bond cleavage which is identified as the rate-determining step. HREELS data suggest different mechanisms for the alkanethiolate decomposition at different coverages. On the unsaturated surface, the C–S bond cleavage is followed by β-hydrogen elimination leading to the formation of corresponding terminal alkene (C_nH_{2n}) and surface hydrogen. Part of the alkene molecules interact with reactive iron sites and further decompose to surface hydrocarbon species and surface carbon, while the rest of the alkene desorbs into the gas phase. For the thiol-saturated surface, corresponding alkane (C_nH_{2n+2}) is also observed in the gas phase. At this coverage, further decomposition of the hydrocarbons on the surface is prohibited by the passivation effect of the coadsorbed species. At saturation coverage, the decomposition of alkanethiolate overlayers leave $c(2\times2)$ sulfur overlayers corresponding to 0.5 monolayer of sulfur on the Fe(100) surface. The decomposition of all the alkanethiol molecules studied here occurs at the same temperature, indicating that the reactivity of the metal substrate is critical to the bonding interactions at the interface.

Introduction

Corrosion of iron and steel is a major concern in the petrochemical industry, due to the destructive attack of iron substrates by chemical and electrochemical reactions involving a variety of species found in hydrocarbon production reservoirs.[1] One common approach to control such corrosion is to add small amounts of organic compounds (inhibitors) to the production fluid.[2] The organic molecules are believed to form protective overlayers on the exposed metal surfaces.[3] While many organic inhibitors are in use today, they have limitations with respect to operating temperature and chemical aggressivity of the corrosive medium. Novel inhibitors that provide increased corrosion resistance to iron-based materials are therefore very desirable. Although current inhibition technology has employed a combination of scientific intuition and empirical approach to develop a number of successful corrosion-inhibitor systems, the interactions between metal substrate and inhibitors are not very well understood. A molecular level understanding of metal–inhibitor interactions can provide insights into the design of inhibitor systems with superior properties.

During the past decade, the reaction of alkanethiols and the formation of stable "self-assembled" alkanethiol monolayers on various transition-metal surfaces have drawn wide attention. These studies have been motivated by the technological promises of ultrathin organic films in the fields of microelectronics, nonlinear optics, electrochemistry, biosensors, wetting, adhesion, and corrosion control as well.[4–6] It is well-known that alkanethiol molecules can form well-ordered, relatively stable adlayers on noble transition metals such as Au.[7–10] Increasing the length of the hydrocarbon alkane chain has been found to significantly enhance the stability and ordering of the overlayer due to hydrophobic interchain attractions. Such systems, which can be viewed as two-dimensional crystals, are often referred to as self-assembled monolayers (SAMs). It has been

* To whom correspondence should be addressed.

[⊗] Abstract published in *Advance ACS Abstracts,* August 15, 1995.

(1) Ramanarayanan, T. A.; Smith, S. N. *Corrosion* **1990**, *46*, 66.

(2) Uhlig, H. H.; Revie, R. W. *Corrosion and Corrosion Control*, 3 ed.; John Wiley & Sons: New York, 1985.

(3) Schweitzer, P. A. In *Corrosion and Corrosion Protection Handbook*, 2 ed.; Schweitzer, P. A., Ed.; Marcel Dekker: New York, 1988; p 660.

(4) Swallen, J. D.; Allara, D. L.; Andrade, J. D.; Chandross, E. A.; Garoff, S.; Israelachvili, J.; McCarthy, T. J.; Murray, R.; Pease, R. F.; Rabolt, J. F.; Wynne, K. J.; Hu, H. *Langmuir* **1987**, *3*, 932–950.

(5) Ulman, A. *An Introduction to Ultrathin Organic Films: From Langmuir-Blodgett to Self-Assembly*; Academic Press: San Diego, 1991.

(6) Dubois, L. H.; Nuzzo, R. G. *Annu. Rev. Phys. Chem.* **1992**, *43*, 437.

(7) Strong, L.; Whitesides, G. M. *Langmuir* **1988**, *4*, 546–558.

(8) Whitesides, G. M.; Laibinis, P. E. *Langmuir* **1990**, *6*, 87–96.

(9) Bain, C. D.; Troughton, E. B.; Tao, Y. T.; Evall, J.; Whitesides, G. M.; Nuzzo, R. G. *J. Am. Chem. Soc.* **1989**, *111*, 321–335.

(10) Dubois, L. H.; Zegarski, B. R.; Nuzzo, R. G. *J. Chem. Phys.* **1993**, *98*, 678–688.

0897-4756/95/2807-1807$09.00/0

reported that interfaces of this type serve as tunneling barriers for electron transport.[11,12] The suggestion has also been made that these structures may have an important role in the suppression of corrosion reactions on gold surfaces. It has also been reported that a chemical bond between iron and thiols can be formed if the substrate is free of oxide.[13] In addition, it has been noted that thiols are effective in inhibiting the corrosion of stainless steel in acidic media.[14] Studies of the dissociation of thiols on reactive metal surfaces are therefore critical in providing insights into overlayer formation and film breakdown mechanisms.

Although the detailed reactivity of methanethiol has been studied on a variety of metal surfaces including Pt(111),[15,16] Cu(100),[17] W(211),[18] Fe(100),[19] Ni(111),[20] Ni(100),[21] Ni(110),[22] and Au(111),[23] little work is available on the interaction of reactive metal surfaces with higher molecular weight alkanethiols. For methanethiol on most of these metal surfaces, cleavage of the S–H bond at low temperature results in the formation of a methanethiolate film, except for Au(111), on which methanethiol adsorbs and desorbs molecularly.[23] Further decomposition of the methanethiolate film depends on the metal substrate as well as the methanethiol coverage. Neff and Kitching have studied 1-propanethiol, 1-butanethiol, and other C_3 and C_4 alkanethiols on evaporated nickel films.[24] In these studies, thiolate (R–S–Ni) formation on the surface was observed. Decomposition of the thiolate at 353 K results in the formation of the corresponding olefin and a sulfided nickel surface. Roberts and Friend have investigated ethanethiol[25] and other higher molecular weight alkanethiol molecules[26,27] on the Mo(110) surface. It was found that the alkanethiols underwent dissociative adsorption via S–H bond scission to form surface alkanethiolate which further decomposed to surface sulfur, surface hydrocarbon fragments, and gas-phase hydrocarbons (alkane and alkene). Parker and Gellman[28] have studied the structure and chemistry of 1-alkanethiols with chain lengths from C_1 to C_6 on the Ni(100) surface. Formation of alkanethiolates was also observed. Further decomposition of the thiolate overlayers results in the formation of alkanes, olefins, hydrogen, and surface-adsorbed sulfur. It was suggested that the thiolates are self-assembled on the surface with alkyl chains tilted away from the surface. Very recently, adsorption of ethanethiol on Au(110) and Ag(110) was reported by Jaffey and Madix.[29] In that investigation, a portion of adsorbed ethanethiol was found to form ethanethiolate. The ethanethiolate further decomposes to H_2, H_2S, ethylene, and ethane on both surfaces, while gaseous ethyl disulfide was also detected from the Au(110) surface.

In a previous paper,[30] we reported the decomposition of ethanethiol on the clean Fe(100) surface. It was found that ethanethiol undergoes S–H bond cleavage to form ethanethiolate upon adsorption at 100 K. The ethanethiolate film mainly decomposes to surface sulfur, gaseous ethylene, and hydrogen. At low coverage, partial decomposition of ethylene on the surface was also observed. At high coverage, however, ethylene decomposition is not seen. Instead, a fraction of the adsorbed ethyl group recombines with surface hydrogen to form ethane.

In the present investigation, the adsorption and decomposition of higher molecular weight alkanethiols (1-butanethiol, 1-hexanethiol, and 1-decanethiol) on the Fe(100) surface has been studied using temperature-programmed reaction spectroscopy (TPRS). Auger electron spectroscopy (AES), low-energy electron diffraction (LEED), and high-resolution electron energy loss spectroscopy (HREELS). Reaction mechanisms are proposed to elucidate the decomposition processes. These results indicate that the reactivity of the substrate is critical to the stability of the interface, affecting the reactivity of the thiol C–S bond. In contrast to the reported interactions between alkanethiols and gold surfaces, increasing the hydrocarbon chain length above C_2 is not effective in enhancing the stability of alkanethiol films on reactive substrates such as iron.

Experimental Section

The experiments were performed in an ion-pumped stainless steel ultrahigh-vacuum chamber equipped with facilities for AES, LEED, TPRS, and HREELS measurements. The base pressure of the system was kept below 2×10^{-10} Torr.

The Fe crystal spot-welded to two tantalum wires was mounted on an off-axis manipulator. The temperature of the sample could be adjusted from 100 to 950 K by a combination of liquid nitrogen cooling and electrical resistive heating. The Fe(100) surface was cleaned by repeated argon ion sputtering followed by annealing under vacuum. The surface cleanliness was checked by AES and HREELS, and the crystallographic order was verified by LEED.

Gases were admitted into the vacuum chamber through a doser attached to a Varian adjustable leak valve. The exposures were measured in langmuir (1 langmuir = 10^{-6} Torr s) using an ion gauge to monitor the pressure in the chamber. 1-Butanethiol (Aldrich 99%), 1-hexanethiol (95%), and 1-decanethiol (96%) were dried over type 4A molecular sieves and degassed by several freeze–pump–thaw cycles prior to use.

The TPRS measurements were carried out at an initial adsorption temperature of 100 K. The TPRS spectra were recorded by placing the crystal in front of the quadrupole mass spectrometer and linearly ramping the crystal temperature at 10 K/s. The mass spectrometer ionizer is enclosed in a thin metal cylinder (2 in. diameter) with a coaxial entrance aperture (1/4 in. diameter). This shield serves to reduce the

(11) Porter, M. D.; Bright, T. B.; Allara, D. L.; Chidsey, C. E. D. *J. Am. Chem. Soc.* **1987**, *109*, 3559–3568.
(12) Chidsey, C. E. D.; Loiacono, D. L. *Langmuir* **1990**, 682–691.
(13) Volmer-Uebing, M.; Stratmann, M. *Appl. Surf. Sci.* **1992**, *55*, 19–35.
(14) Saleh, J. M.; Al-Haidari, Y. K. *Bull. Chem. Soc. Jpn.* **1989**, *62*, 1237–1245.
(15) Koestner, R. J.; Stohr, J.; Gland, J. L.; Kollin, E. B.; Sette, F. *Chem. Phys. Lett.* **1985**, *120*, 285–291.
(16) Rufael, T. S.; Koestner, R. J.; Kollin, E. B.; Salmeron, M.; Gland, J. L. *Surf. Sci.* **1993**, *297*, 272–285.
(17) Sexton, B. A.; Nyberg, G. L. *Surf. Sci.* **1986**, *165*, 251–267.
(18) Benziger, J.; Preston, R. E. *J. Phys. Chem.* **1985**, *89*, 5002–5010.
(19) Albert, M. R.; Lu, J. P.; Bernasek, S. L.; Cameron, S. D.; Gland, J. L. *Surf. Sci.* **1988**, *206*, 348–364.
(20) Castro, M. E.; White, J. M. *Surf. Sci.* **1991**, 22–32.
(21) Castro, M. E.; Ahkter, S.; Golchet, A.; White, J. M. *Langmuir* **1991**, *7*, 126–133.
(22) Huntley, D. R. *J. Phys. Chem.* **1989**, *93*, 6156–6164.
(23) Nuzzo, R. G.; Zegarski, B. R.; Dubois, L. H. *J. Am. Chem. Soc.* **1987**, *109*, 733–740.
(24) Neff, L. D.; Kitching, S. C. *J. Phys. Chem.* **1974**, *78*, 1648–1653.
(25) Roberts, J. T.; Friend, C. M. *J. Phys. Chem.* **1988**, *92*, 5205–5213.
(26) Roberts, J. T.; Friend, C. M. *J. Am. Chem. Soc.* **1986**, *108*, 7204–7210.
(27) Roberts, J. T.; Friend, C. M. *J. Am. Chem. Soc.* **1987**, *109*, 3872–3882.
(28) Parker, B.; Gellman, A. J. *Surf. Sci.* **1993**, *292*, 223–234.
(29) Jaffey, D. M.; Madix, R. J. *Surf. Sci.* **1994**, *311*, 159–171.
(30) Cheng, L. C.; Bocarsly, A. B.; Bernasek, S. L.; Ramanarayanan, T. A. *Langmuir* **1994**, *10*, 4542–4550.

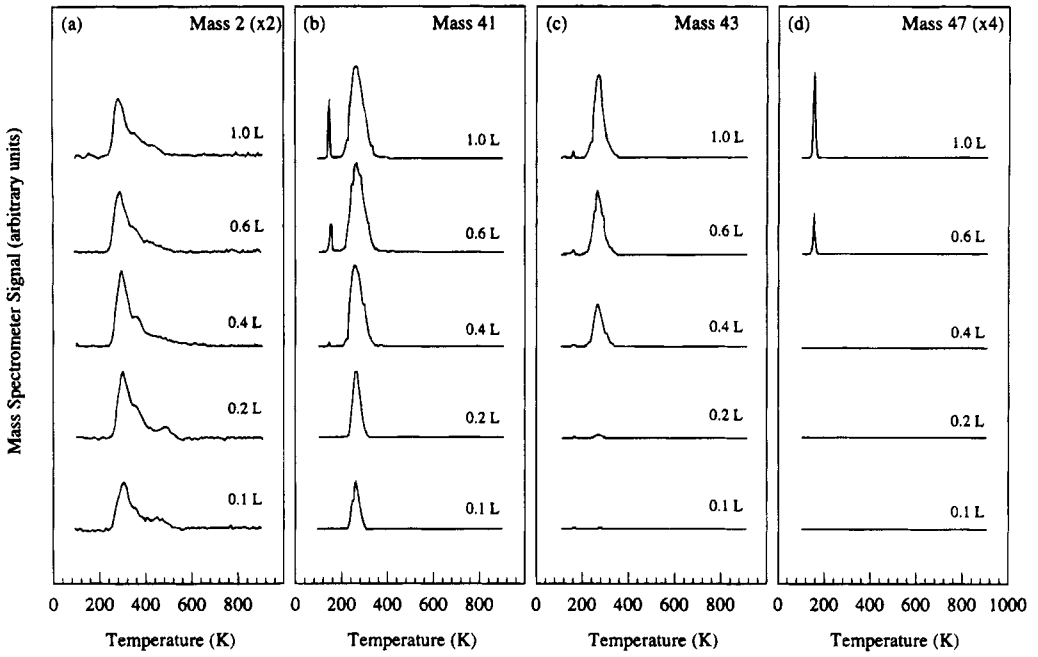

Figure 1. TPRS of 1-butanethiol on the Fe(100) surface as a function of 1-butanethiol exposure: (a) hydrogen; (b) butene; (c) butane; (d) 1-butanethiol. Vertical scale expansion factors of mass 2 and 47 are referenced to mass 41 and 43. The data shown are not corrected for alkane fragmentation.

signal from background gas desorption and to prevent electron impact on the surface. The signal-to-noise ratio of the mass spectrometer is greater than 100. The HREELS monochromator and analyzer were both 127° cylindrical sectors. The vibrational spectra were collected under an incident electron beam energy of 5.0 eV. The full width at half-maximum (fwhm) of the elastic peak from the clean Fe(100) was typically 70 cm^{-1}. All the HREELS spectra were recorded at 100 K. Data acquisition for HREELS, TPRS, and AES was accomplished with an IBM-PC-AT interfaced to the spectrometers. The software used has been described elsewhere.[19]

Results

1-Butanethiol. Figure 1 shows the temperature-programmed reaction spectra obtained for 1-butanethiol on the Fe(100) surface as a function of thiol exposure. Hydrogen evolution (mass 2) is depicted in Figure 1a, and three hydrocarbon fragments are presented in Figure 1b–d. Two desorption peaks for hydrocarbon fragments were observed in the TPRS at 260 and 150 K. The maximum desorption temperature for both peaks remains nearly the same with increasing exposure. To determine the gas phase products, TPRS experiments were performed for all the *m/e* units in the region between 2 and 200. Figure 2 shows the results of the intensity for the peaks detected at 260 K. The intensities were obtained by integrating the area under each spectrum between 180 and 600 K. Since our mass spectrometer detects 10 mass units at a time, the mass 41 peak was kept as an internal standard for intensity calibration. Masses 56, 41, 40, 39, 29, 28, 27, 26, and 15 are seen at all the exposures. Their intensities increase with 1-butanethiol exposure. At exposures below 0.4 langmuir, mass 43 can also be seen but the intensity is very weak. When the exposure reaches 0.4 langmuir and higher, the mass 43 peak intensity increases dramatically, while another peak at mass 58 appears at exposures above 0.2 langmuir.

In determining the identity of the gas-phase products, our previous study on the decomposition of ethanethiol on the Fe(100) surface provides an indication for what could happen here. As previously reported,[30] ethaneth-

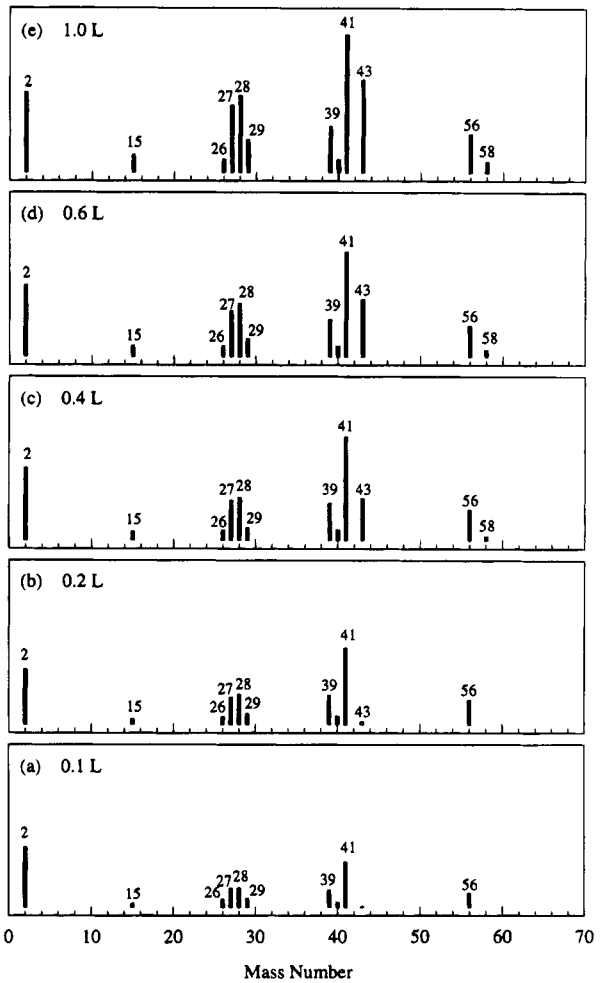

Figure 2. Mass spectra of the gas-phase products during 1-butanethiol decomposition on Fe(100) surface at 260 K as a function of 1-butanethiol exposure: (a) 0.1, (b) 0.2, (c) 0.4, (d) 0.6, and (e) 1.0 langmuir.

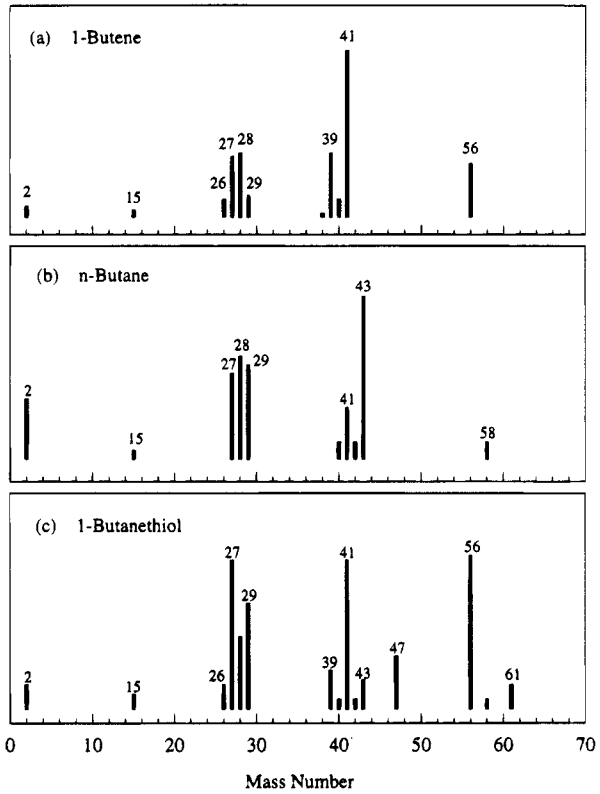

Figure 3. Mass spectra of (a) 1-butene, (b) *n*-butane, and (c) 1-butanethiol recorded with the experimental apparatus used in this investigation.

iol decomposes on the Fe(100) surface to yield ethane and ethylene depending on initial coverages. β-Hydrogen elimination leads to the cleavage of the ethanethiolate C–S bond, producing ethylene as the major product. Only at saturation exposure, another reaction channel opens for ethane formation via the recombination of adsorbed ethyl group and surface hydrogen. Assuming that the interaction of 1-butanethiol with the Fe(100) surface is analogous to that of ethanethiol, the reaction products would be 1-butene and *n*-butane. This is a reasonable prediction as 1-butene and *n*-butane are the products for 1-butanethiol decomposition on the Mo(110)[26] and Ni(100)[28] surface.

To confirm this hypothesis, mass spectra of authentic 1-butene, *n*-butane, and 1-butanethiol were taken using the experimental apparatus in this work. Comparing Figure 2a,b to the spectra of 1-butene (Figure 3a), it can be seen that the reaction product is very likely to be butene. The mass spectrum of *n*-butane (Figure 3b) is very different from that of butene. There are peaks at mass 58 and mass 43, but mass 56 is absent. The appearance of mass 43 and 58 peaks in Figure 2c–e are in good agreement with the formation of *n*-butane at high butanethiol exposures. The mass 56 peak is likely due to both the butene and butane spectra. To test this idea, the spectra in Figure 2 were corrected by subtracting the 1-butene contribution. The result is presented in Figure 4. At exposures of 0.1 and 0.2 langmuir (Figure 4a,b), the corrected spectra show very low intensity for all hydrocarbon fragments, indicating that 1-butene is indeed the gas-phase product at low exposure. At higher exposure, the corrected patterns shown in Figure 4c–e match the *n*-butane spectrum in Figure 3b, except that mass 40 and 42 are not seen. This is probably due to low *n*-butane concentration.

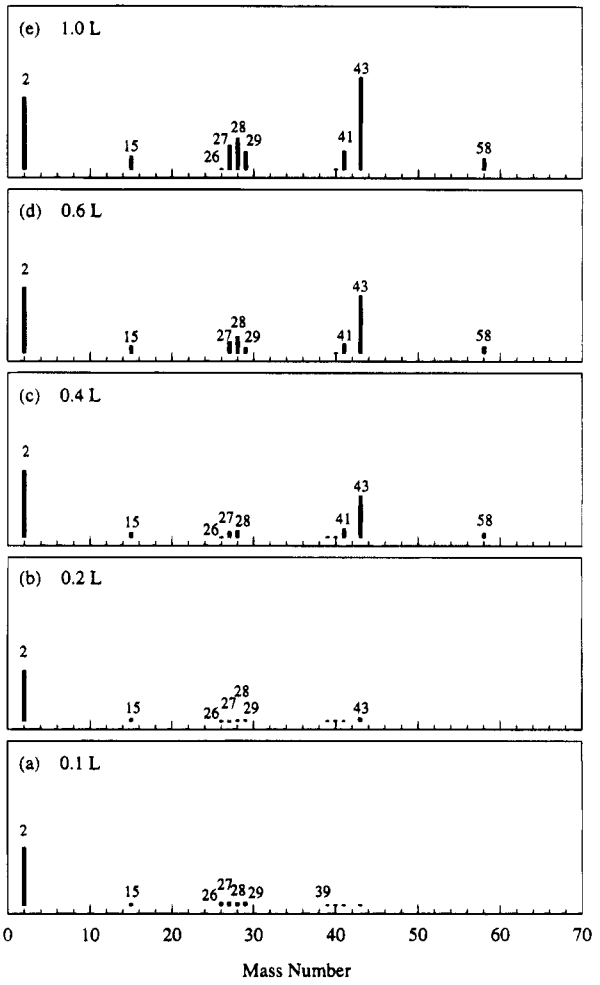

Figure 4. Mass spectra of 1-butanethiol decomposition on the Fe(100) surface at 260 K after subtracting the butene contribution from Figure 2.

Compared to the mass spectra of butene and butane, the mass spectra of 1-butanethiol (Figure 3c) shows two characteristic fragmentations, mass 47 and 61. These two peaks are not observed in the temperature-programmed reaction spectra shown in Figures 2 and 4. Thus, the desorption of intact 1-butanethiol molecules within this temperature region can be ruled out. However, 1-butanethiol parent molecules were observed to desorb in the low-temperature region. Integrating the peaks at 150 K for exposures higher than 0.6 langmuir results in spectra (not shown) similar to 1-butanethiol (Figure 3c). On the basis of this product analysis, masses 2, 41, 43, and 47 are presented in Figure 1 which are representative of the thermal desorption of hydrogen, 1-butene, *n*-butane, and 1-butanethiol, respectively.

Now that the gas-phase products are identified, the TPRS of 1-butanethiol (Figure 1) can be discussed in more detail. Below 0.4 langmuir, 1-butene is the only hydrocarbon product detected in the gas phase. Its desorption temperature is 260 K. Increasing exposure results in butane desorption at the same temperature. At saturation exposure, 1-butanethiol parent molecules desorb at 150 K with a shape and behavior consistent with zero-order desorption kinetics, indicating multilayer adsorption. The sharp peak seen at 150 K for mass 47 is apparently due to the fragmentation of 1-butanethiol multilayer. Hydrogen desorption peaks

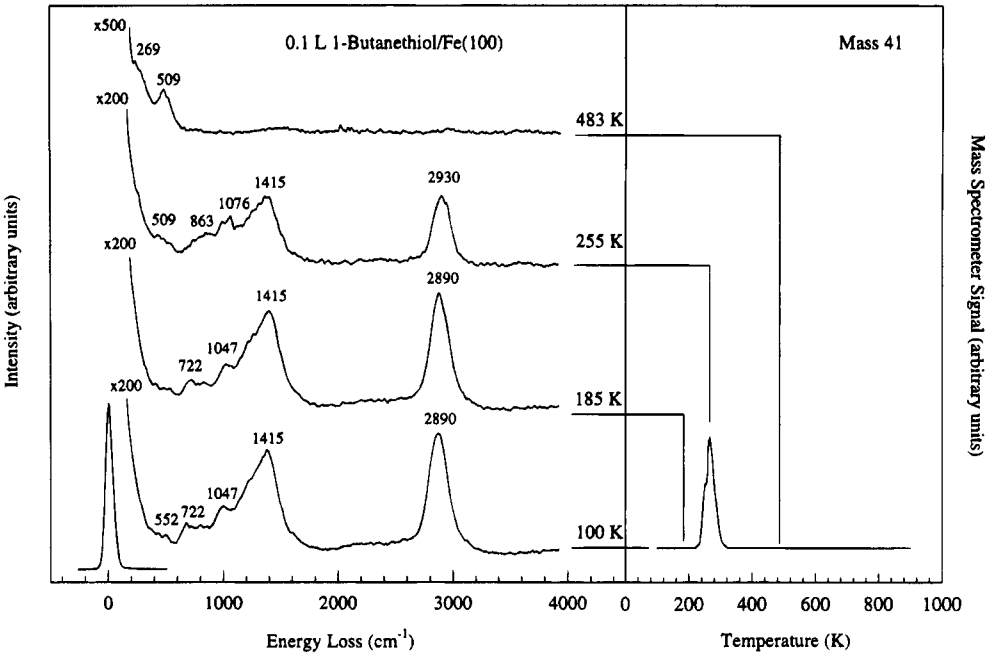

Figure 5. HREELS spectra (left panel) as a function of annealing temperature and TPRS (right panel) after the adsorption of 0.1 langmuir 1-butanethiol on the Fe(100) at 100 K. All spectra were recorded at 100 K after flashing to the indicated temperature.

(Figure 1a) are centered at 300 K with a shoulder at 360 K, similar to the β_1 and β_2 states for the recombination and desorption of hydrogen from the clean Fe(100) surface.[31] At low exposure, however, a small peak at ~500 K is also evident. This temperature is higher than the β_2 state, suggesting that the high-temperature feature is reaction limited and is attributed to the dehydrogenation of hydrocarbon species formed from the thiol decomposition.

HREELS spectra were taken at various temperatures for 1-butanethiol adsorption on the Fe(100) surface according to the TPRS results. Although the resolution of the spectrometer limits the observation of detailed vibrational features, information on adsorption and decomposition can still be obtained. Peak assignments are made by comparing the HREELS to the infrared data for liquid 1-butanethiol.[32] Figure 5 (left panel) shows the HREELS for 1-butanethiol on Fe(100) at low coverage. Upon adsorption at 100 K, a loss peak at 2890 cm^{-1} is assigned to the C–H stretching mode and multiple loss peaks between 722 and 1415 cm^{-1} are attributed to the vibrations of the CH_2 units on the chain. The absence of any energy loss near 2500 cm^{-1} suggests that 1-butanethiol dissociatively adsorbs on the Fe(100) surface via S–H bond cleavage. This is similar to what is observed for 1-butanethiol on the Mo(110) surface[26] and for ethanethiol on the Fe(100) surface,[30] where butanethiolate or ethanethiolate is formed. The C–S stretch at frequencies below 700 cm^{-1} is not evident, probably due to its low intensity. At 185 K, there is no significant change in the HREELS spectrum. By warming up to 255 K, the temperature where butene evolution is detected, the peak at 2890 cm^{-1} shifts to somewhat higher frequency. Meanwhile, new peaks at 509 and 863 cm^{-1} are clearly seen. The peak at 509 cm^{-1} is typically a Fe–C stretch,[33] indicating that the decomposition of hydrocarbons on the Fe(100) surface also occurs. Heating the surface to 483 K results in two bands at 269 and 509 cm^{-1}, which are characteristic of residual atomic sulfur and carbon on the Fe(100) surface.[19,33]

Figure 6 demonstrates the vibrational spectra of 1-butanethiol at saturation coverage. In addition to the C–H stretch at 2909 cm^{-1} and CH_2 vibrational bands between 743 and 1444 cm^{-1}, a loss peak at 2576 cm^{-1} is also observed. This loss energy is in agreement with that for the S–H stretch in liquid 1-butanethiol. Following annealing the surface to 185 K, the absence of this S–H stretching mode suggests that 1-butanethiol adsorbs molecularly during multilayer formation. The C–H stretch and CH_2 vibrational bands remain nearly the same at this temperature. Upon heating the surface further to 255 K, all bands shift to slightly lower frequency. Interestingly, the Fe–C stretch is not observed in this case. At higher temperature (483 K), only one band is seen at 269 cm^{-1} which corresponds to the Fe–S stretch.

After the thermal desorption from the saturated surface, AES gives no indication of carbon on the iron surface which is in good agreement with the TPRS and HREELS results. The saturation coverage is determined to be 0.5 monolayer by the Auger peak-to-peak height ratio of the sulfur KLL line (154 eV) to the iron LMM line (662 eV). This surface shows a clear $c(2\times2)$ LEED pattern, which is similar to that after methanethiol[19] and ethanethiol[30] decomposition at saturation coverage.

1-Hexanethiol and 1-Decanethiol. Figure 7 shows the temperature-programmed reaction spectra for 1-hexanethiol on the Fe(100) surface. Organic products in the gas phase were detected and identified as indicated in the discussion of 1-butanethiol above. Masses 84, 86, and 47 are characteristic fragments for hexene, hexane, and 1-hexanethiol, respectively. When surface satura-

(31) Bozso, F.; Ertl, G.; Grunze, M.; Weiss, M. *Appl. Surf. Sci.* **1977**, *1*, 103–108.
(32) Trotter, I. F.; Thompson, H. W. *J. Chem. Soc.* **1946**, 481.
(33) Lu, J. P.; Albert, M. R.; Chang, C. C.; Bernasek, S. L. *Surf. Sci.* **1990**, *227*, 317.

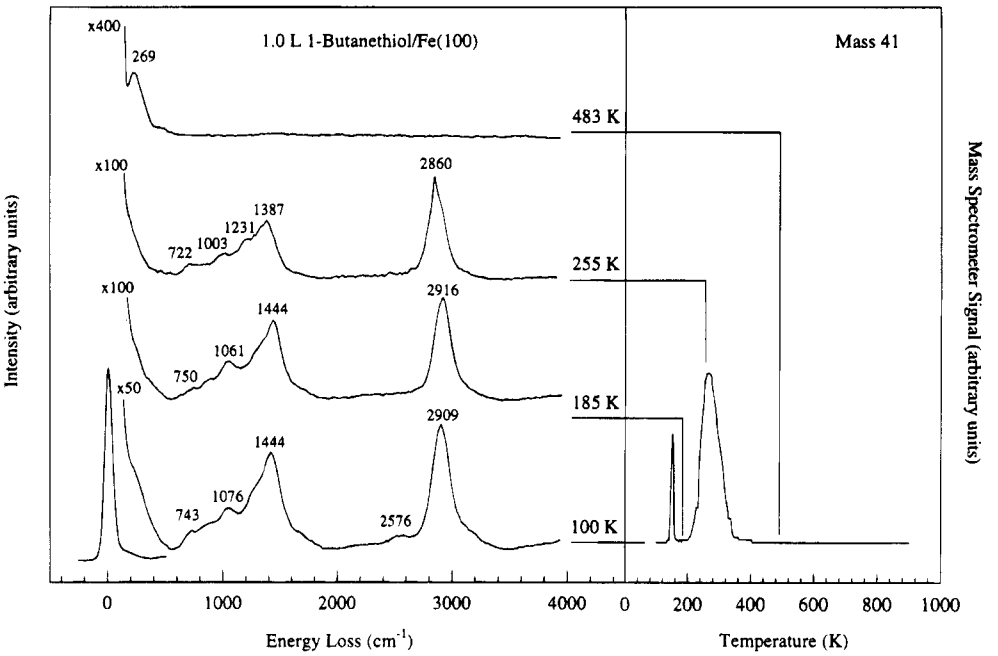

Figure 6. HREELS spectra (right panel) as a function of annealing temperature and TPRS (right panel) after the adsorption of 0.1 langmuir 1-butanethiol on the Fe(100) at 100 K. All spectra were recorded at 100 K after flashing to the indicated temperature.

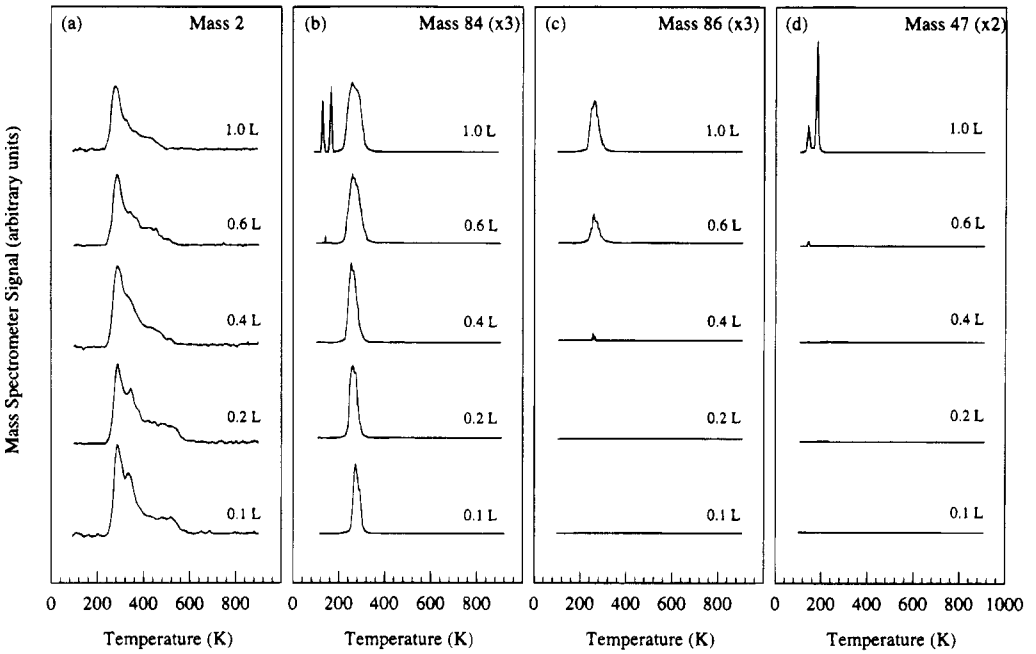

Figure 7. TPRS of 1-hexanethiol on the Fe(100) surface as a function of 1-hexanethiol exposure: (a) hydrogen; (b) hexene; (c) hexane; (d) 1-hexanethiol. The data shown are not corrected for alkane fragmentation.

tion is reached at 0.6 langmuir, molecular desorption of 1-hexanethiol (Figure 7d) is observed at 140 K. At 1.0 langmuir exposure, another peak also appears at 175 K with strong intensity, while the peak intensity at 140 K increases. Both peaks are sharp with behavior suggestive of multilayer desorption. This is probably due to the coexistence of two phases in the multilayer. As thiol exposure increases, part of the intact molecules may crystallize to form an ordered structure while the rest still remain disordered, resulting in two multilayer desorption states. Hexene evolution is observed at 260 K at exposures between 0.1 and 1.0 langmuir (Figure 7b). The low-temperature peaks appearing at saturation coverages are attributed to the cracking of 1-hexanethiol. At high exposures, hexane is also detected evolving at 260 K (Figure 7c). TPRS for hydrogen in Figure 6a shows that desorption peaks are centered at 300 K with a shoulder at 380 K tailing up to 500 K. At low exposures, there is a high-temperature feature for hydrogen evolution at >500 K. As with 1-butanethiol, this peak is due to the decomposition of surface hydrocarbon fragments.

Figure 8 depicts the temperature-programmed reaction spectra of 1-decanethiol on the Fe(100) surface. Masses 41, 43, and 47 are selected to demonstrate decene, decane, and 1-decanethiol evolution, respectively. As can be seen in Figure 8d, 1-decanethiol parent molecules desorb from the surface at high exposures. Multiple desorption states are seen at 112, 140, and 175 K. The fragmentation of the parent

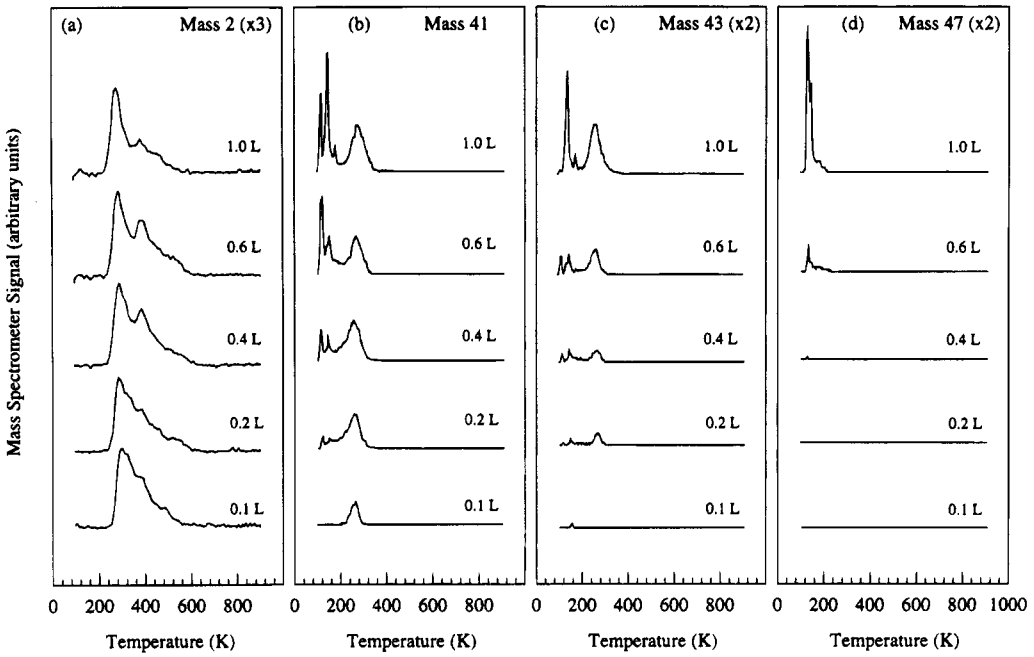

Figure 8. TPRS of 1-decanethiol on the Fe(100) surface as a function of 1-decanethiol exposure: (a) hydrogen; (b) decene; (c) decane; (d) 1-decanethiol. The data shown are not corrected for alkane fragmentation.

molecule results in the features at the same temperature in Figure 8b,c. It can also be seen in Figure 7b,c that the decomposition of 1-decanethiol occurs at 260 K, producing decene and decane. TPRS for hydrogen are similar to that for 1-hexanethiol except that the peaks are broadened and more total hydrogen is evolved.

Decomposition of fully saturated 1-hexanethiol and 1-decanethiol leaves 0.5 monolayer of sulfur on the Fe(100) surface as determined by AES. LEED measurements show a sharp $c(2\times2)$ pattern which is identical to 1-butanethiol decomposition as well as those from ethanethiol[30] and methanethiol[19] on the same iron surface. Temperature-dependent HREELS spectra for both unsaturated and saturated overlayer are also very similar to those of 1-butanethiol. For the unsaturated surface, the S–H stretch at ~2500 cm^{-1} was not observed at 100 K, suggesting S–H scission upon adsorption. Heating the surface to higher temperature results in the formation of surface hydrocarbon fragments as indicated by the intense Fe–C stretching mode at ~510 cm^{-1}. After the total decomposition, HREELS shows energy losses at 269 and 510 cm^{-1} due to surface sulfur and carbon adatoms. At saturation coverage, an S–H stretch was observed for the multilayer alkanethiols. This mode disappears after multilayer desorption, indicating the formation of an alkanethiolate overlayer. Annealing the surface in the region between 100 and 483 K, no evidence for surface hydrocarbon fragments was seen. Fe–S stretch at 269 cm^{-1} is the only loss peak after the decomposition of saturated 1-hexanethiolate and 1-decanethiolate at 483 K.

Discussion

Adsorption of 1-Alkanethiol on Clean Fe(100) Surface. As indicated by the spectroscopic data shown in the previous section, 1-butanethiol, 1-hexanethiol, and 1-decanethiol dissociatively adsorb on the Fe(100) surface at temperatures as low as 100 K. The S–H bond scission with low activation energy[25] was observed previously for methanethiol and ethanethiol on the Fe(100) surface.[19,30] In those cases, the S–H bond cleavage leads to the formation of methanethiolate and ethanethiolate on the Fe(100) surface. Similar behavior on various transition-metal surfaces has also been reported. For thiols on the Ni(100)[28] and Mo(110)[25-27] surface, for example, the scission of the S–H bond results in the formation of thiolate (e.g., ethanethiolate for ethanethiol and butanethiolate for butanethiol). As determined by TPRS, AES, LEED, and HREELS, the saturation coverage of the alkanethiolate overlayer is 0.5 monolayer for 1-butanethiol, 1-hexanethiol, and 1-decanethiol, where 1 monolayer is defined as the number of iron atoms in the topmost layer of the Fe(100) surface. This saturation coverage is equivalent to that of methanethiol and ethanethiol adsorption on the Fe(100) surface,[19,30] suggesting that the hydrocarbon chain length does not affect the packing density of the alkanethiolates on the Fe(100) surface. While the interaction between the sulfur and the iron substrate provides an anchor for the thiolate to the surface, the hydrocarbon chains tend to point toward the surface normal due to hydrophobic interaction of the hydrocarbon chains, similar to that observed for alkanethiolates on the Ni(100) surface.[28]

Thermal Decomposition of Alkanethiolate. Like ethanethiol, 1-butanethiol, 1-hexanethiol, and 1-decanethiol decompose on the Fe(100) surface at 260 K. Figure 9 outlines the mechanism for the adsorption and decomposition of the alkanethiols on the Fe(100) surface based on the spectroscopic information.

As the TPRS results indicate, alkenes and alkanes are the major hydrocarbon products in the gas phase. Therefore the decomposition occurs via C–S bond activation. After the C–S bond cleavage, further decomposition is coverage dependent as shown in the HREELS data. At lower coverage, two competing reaction pathways are involved in the further reaction process. One is the direct evolution of unsaturated hydrocarbons (butene, hexene, or decene) to the gas phase, presumably following β-hydrogen elimination.

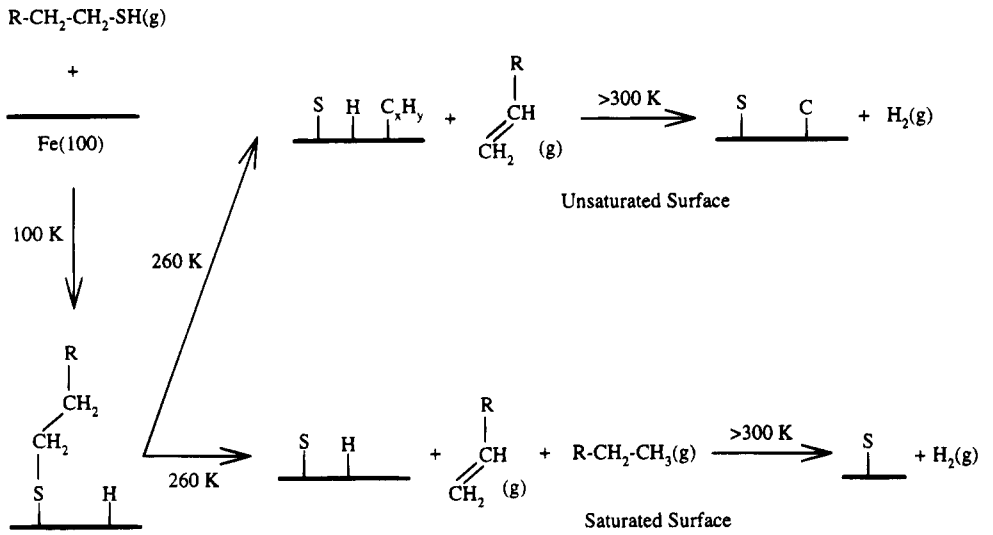

Figure 9. Proposed mechanism for the adsorption and decomposition of 1-alkanethiols on the Fe(100) surface.

The other is the total decomposition of a fraction of the hydrocarbon molecules on the surface. This is supported by the Fe–C stretch observed in the HREELS above 255 K, although the surface hydrocarbon species cannot be clearly identified. Further decomposition of the surface hydrocarbon species results in hydrogen desorption at higher temperature and surface-bound carbon atoms.

At saturation coverage, however, the reaction kinetics is altered. While the evolution of alkene persists, decomposition of hydrocarbon on the surface is evidently prohibited, since no iron–carbon stretch was observed during and after the decomposition process. The Fe–S stretch is observed as the only vibrational mode after the decomposition is completed at 483 K. In addition, saturated hydrocarbons such as butane, hexane, and decane are formed by hydrogen abstraction from the surface.

It can be concluded that the decomposition of the 1-alkanethiolate overlayer is limited by the C–S bond cleavage at both low and high coverages. This step is followed by three reaction pathways: alkene formation, alkene decomposition, and alkane evolution. Among these, alkene formation is the predominant reaction pathway. This process, via β-hydrogen elimination, is kinetically favorable. Alkene decomposition and alkane evolution, however, are dependent on the alkanethiolate coverage. This is evident in the hydrogen TPRS (Figure 1a), where the hydrogen peak intensity does not change dramatically as the thiol exposure increases. In fact, the decomposition of alkene results in high-temperature desorption and a relatively higher surface hydrogen concentration at lower alkanethiol exposure. Huntley[22] demonstrated that surface electronegative modifiers such as S and O could alter the reaction pathway. In that investigation of methanethiol decomposition on the Ni(110) surface, S or O caused a stabilization of the thiolate species with respect to decomposition and an increase in the methane yield. It is reasonable to propose that in the present case the surface coadsorbates could stabilize the neighboring surface alkanethiolate group. At less than saturation coverage, there are "open" iron sites which may serve as a reaction catalyst. These reactive sites are effectively blocked by the coadsorbates such as alkanethiolate at saturation coverage. Therefore, the iron surface is passivated and the formation of surface hydrocarbon fragments is prohibited. The passivation effect opens the pathway for the alkyl group to combine with surface hydrogen to produce alkane.

Decomposition Temperature. The decomposition temperature of 1-alkanethiol on the Fe(100) surface (260 K) is lower than that found for methanethiol on various transition-metal surfaces such as W(211) (410 K),[18] Cu(100) (370 K),[17] Ni(100) (270 K),[21] and Pt(111) (>300 K)[16] surfaces. It is also lower than that for the 1-butanethiol molecule on the Mo(110) surface (305 K for butane and 355 K for butene).[26] This is perhaps due to the reactivity of iron that weakens the bonding in the alkanethiolate film. It is noted that the decomposition temperature for these alkanethiols is also lower than that for methanethiol on the same Fe(100) surface.[19] The difference in the decomposition temperature could also result from kinetic effects. While alkanethiolates with two or more carbon atoms on the chain can undergo β-hydrogen elimination, the methanethiolate undergoes C–S bond scission, followed by methyl group and surface hydrogen recombination. Although long-chain alkanethiols form stable layers at room temperature on some of the transition-metal surfaces, this is not the case for iron, likely due to the reactivity of iron in activating C–S bond scission. Figure 10 summarizes the decomposition temperature of these alkanethiols as a function of the number of carbon atoms in the chain. The molecules with longer hydrocarbon chains decompose at the same temperature as ethanethiol. This behavior is very different from that reported on the gold surface. Clearly the reactivity of the substrate affects the bonding interactions at the interface. For methanethiol on iron and gold, for example, the iron–sulfur bond is stronger than the gold–sulfur bond. The C–S stretching frequency on iron is 601 cm^{-1} which is lower than that on gold (700 cm^{-1}). This means that iron interacts more strongly with the thiols than does gold. In addition, β-hydrogen elimination as was observed in the decomposition of the ethanethiol is a kinetically favorable pathway for the longer chain alkanethiols as well.

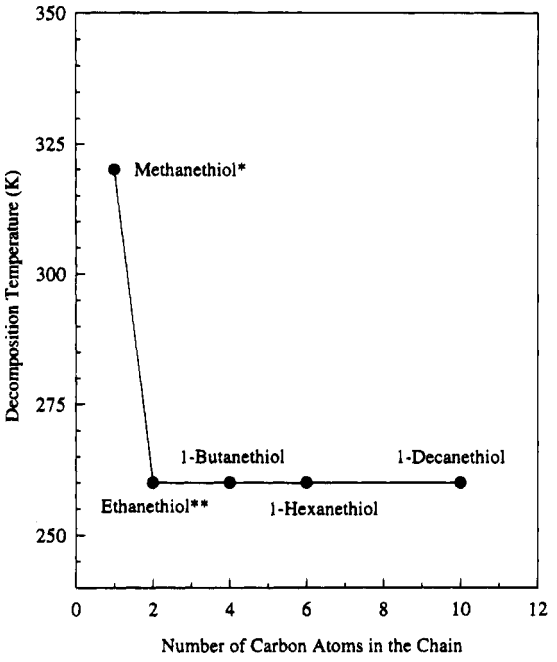

Figure 10. Decomposition temperature of 1-alkanethiol molecules on Fe(100) surface: (*) value is from ref 19; (**) value is from ref 30.

Conclusion

The results presented in this investigation address some important questions concerning the adsorption and decomposition of alkanethiols on the Fe(100) surface. Alkanethiol dissociatively adsorbs on the Fe(100) surface at 100 K. Cleavage of the S–H bond leads to the formation of surface hydrogen and surface 1-alkanethiolate. Saturation coverage corresponds to 0.5 monolayer. Higher exposure results in multilayer alkanethiol adsorption. At temperatures <253 K, surface alkanethiolate starts to decompose to gas-phase hydrocarbons, surface sulfur, and surface hydrocarbon fragments depending on the alkanethiolate coverage. Alkene is the major product during the thermal decomposition, via C–S bond cleavage and β-hydrogen elimination. At less than saturation coverage, hydrocarbon decomposition on the iron surface competes with alkene desorption due to the availability of reactive iron sites. At saturation coverage, coadsorbates on the Fe(100) surface passivate the iron surface and stabilize the hydrocarbon group. Decomposition of hydrocarbons on the surface is greatly restricted. This effect favors alkane formation near saturation coverage. Strong iron–sulfur interaction weakens the C–S bond, leading to the decomposition of the alkyl thiolate at a lower temperature on iron than on many other transition metals. The elimination of β-hydrogen provides a kinetically favorable pathway for long-chain alkanethiolate dissociation on iron. Due to the strong interaction between the substrate and alkanethiol molecules as well as the β-elimination process, longer hydrocarbon chains do not enhance the stability of alkanethiols on the Fe(100) surface, in contrast to what has been proposed for these self-assembled monolayers on noble metal surfaces such as gold.[7–10]

Acknowledgment. Partial support of this research by Exxon Research and Engineering Co. is gratefully acknowledged.

CM940557B